

Three-dimensional instability of anticyclonic swirling flow in rotating fluid: Laboratory experiments and related theoretical predictions

Ya. D. Afanasyev and W. R. Peltier

Department of Physics, University of Toronto, Toronto, Ontario M5S 1A7, Canada

(Received 9 April 1997; accepted 3 September 1998)

We present results from a new series of experiments on the geophysically important issue of the instability of anticyclonic columnar vortices in a rotating fluid in circumstances such that the Rossby number exceeds unity. The core of the vortex is modeled as a solid cylinder rotating in a fluid that is itself initially in a state of solid-body rotation. When the cylinder rotates cyclonically the flow induced by the differential rotation is stable except for a brief initial period. When the cylinder rotates anticyclonically, however, intense perturbations spontaneously appear and amplify in the flow. The experimental results demonstrate that secondary motions appear in an annular region of finite width surrounding the cylinder (in accord with the prediction of the generalized Rayleigh criterion) and are governed by the process of three-dimensional centrifugal instability. These motions are characterized by a definite wave number in the coordinate direction parallel to the axis of the cylinder. Both the width of the unstable annular region and the vertical wavelength of the motions induced by centrifugal instability are determined by the main nondimensional parameter of the flow—the Rossby number. The evolution of the secondary motions gives rise to the appearance of tertiary motions—which are Kelvin–Helmholtz-like (barotropic) vortices that develop at the periphery of the unstable annulus, thus leading to the formation of exceedingly complex dynamical structures. If the rotating cylinder is withdrawn vertically from the fluid, the instability rapidly destroys the core of the vortex. During its initial phase of development the flow evolves in a way that is strongly analogous to the cylindrical Couette case. An appropriate theory is employed to explain the results of the laboratory experiments. © 1998 American Institute of Physics. [S1070-6631(98)02812-8]

I. INTRODUCTION

Compact vortices are abundant in both the atmosphere and the oceans and they play an important role in the global dynamics of these geophysical fluids. The Earth's rotation may, of course, be a crucial factor in determining the initial development of such coherent structures as well as their stability characteristics. Small and mesoscale columnar vortices in middle latitudes as well as larger-scale vortices in equatorial regions may, in particular, be subject to the centrifugal (inertial) instability due to the background rotation, although this fact has only been realized rather recently (see, e.g., Smyth and Peltier,¹ Carnevale *et al.*,² and Potylitsin and Peltier³). An important control parameter in determining the stability of a columnar vortex is clearly the Rossby number, $Ro = \omega/2\Omega_0$, which represents the ratio of vorticity ω in the column to the background vorticity $2\Omega_0$. The behavior of flows for limiting cases in which Ro is either very small or very large, is relatively clear. When $Ro \ll 1$ the background rotation tends to two-dimensionalize (and thus stabilize) the vortical flow, an effect that is well understood on the basis of the Taylor–Proudman theorem. In the opposite limit the flow does not “feel” the rotation at all and there is therefore no essential difference between cyclones and anticyclones. Our intention herein is to focus upon the interesting intermediate regime, namely, that in which $Ro \gtrsim 1$.

Although a small number of recent articles have ap-

peared that have been focused upon the behavior of barotropic vortices in a rotating fluid, this geophysically important problem seems yet to be fully understood. For example, there have appeared several reports of results obtained through direct numerical simulation^{4,5} of various vortical flows that have established that initially two-dimensional anticyclonic vortices may be strongly destabilized by three-dimensional perturbations, whereas cyclonic vortices remain stable when the Rossby number is of order unity. Theoretical analyses by Smyth and Peltier¹ suggested by the numerical simulations by Lesieur *et al.*,⁴ have clearly demonstrated that in the case of an array of elliptic vortices in shear created as a result of Kelvin–Helmholtz instability, the growth rate of a mode (referred to by the authors as the “edge mode”) of instability associated with centrifugal destabilization varies strongly as a function of both the Rossby number and the vertical wave number of the perturbation and reaches a maximum for a value of the Rossby number, that is $O(1)$, when the vortices are anticyclonic. It was shown that kinetic energy for this mode is localized in an elliptic annular region at the periphery of the vortex, where the generalized Rayleigh criterion suggests that centrifugal instability should reside (see also Potylitsin and Peltier³). The difference in the behavior of cyclones and anticyclones has also been demonstrated in the recently described numerical experiments of Carnevale *et al.*² It was shown by these authors that for Rossby numbers greater than one, even small perturbations completely

destroyed the anticyclonic vortex through centrifugal instability, while cyclones remain stable. The influence of rotation on parallel shear flows and mixing layers has been studied experimentally in the recent literature both by Alfredson and Persson⁶ and by Bidokhti and Tritton.⁷ In this work it was found that, whereas regions of cyclonic vorticity have increased stability in the presence of background rotation, regions of anticyclonic vorticity are thereby destabilized. An additional demonstration of the differential behavior of anticyclones and cyclones in a rotating environment was provided by the rotating tank experiments of Kloosterziel and van Heijst.⁸ In their experiments the anticyclones were produced using a gravitational collapse technique and were observed to be destroyed immediately upon generation, whereas cyclones formed in the same way remained stable. When vortices were created by the so-called stirring technique, so that the resulting vortex consisted of a patch of vorticity of one sign surrounded by a ring of opposite vorticity, the vortices with anticyclonic vorticity in the core split into two dipoles that subsequently moved apart. These authors also demonstrated that anticyclonic vortices might be expected to be centrifugally unstable according to an extension of Rayleigh's criterion to rotating flows. However, the details of the evolution of the centrifugal instability and the manner in which the instability destroys the vortex remained unclear. Using a so-called "displaced-particle" technique, Kloosterziel and van Heijst⁸ showed that the classical Rayleigh criterion may be extended in order to include the Coriolis force. In a recent and related theoretical paper by Leblanc and Cambon,⁹ the authors demonstrated that different criteria for inertial instability obtained previously for some planar flows with simple symmetry (e.g., parallel shear flows, circular vortices) can be related via a generalized criterion based on the sign of the second invariant of the "inertial tensor."

The main aim of the present work is to reproduce the evolution of the "edge mode" discovered by Smyth and Peltier¹ experimentally. For this purpose a new sequence of experiments in which the stable core of a barotropic vortex is represented by a rotating solid cylinder has been performed. The cylinder itself was placed in a rotating tank. Instability then can develop in the annular region around the cylinder where the swirling flow induced by the cylinder may be unstable according to the generalized Rayleigh's criterion. In spite of the obvious limitations of such a representation of an unstable vortex, we believe that these experiments do provide considerable insight into the dynamics of the instability of "free" barotropic vortices in a rotating fluid. The advantage of the experimental geometry that we have selected also lies in the fact that this basic state is dynamically similar to the classical Taylor-Couette flow. Theoretical results concerning the nature of the stability of that flow will provide very useful insight into the nature of the mechanism of centrifugal instability through which anticyclones may be preferentially destabilized in the presence of rotation in the regime in which the Rossby number is of order unity.

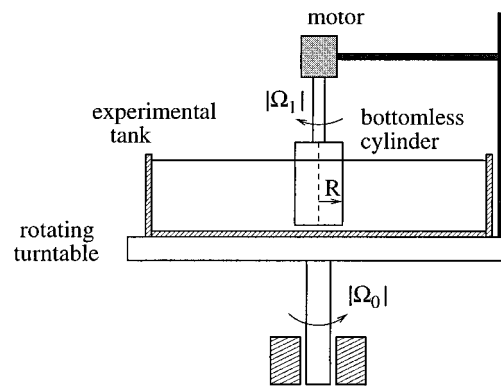


FIG. 1. Sketch of the experimental apparatus.

II. LABORATORY APPARATUS AND TECHNIQUE

Our experiments were carried out in a rectangular Perspex tank of dimensions $80 \times 80 \times 15$ cm mounted on a rotating turntable (Fig. 1). The tank was rotated about a vertical axis through its center in an anticlockwise direction with the rotation rate Ω_0 between 0.03 and 0.4 s^{-1} . The tank itself was filled with a homogeneous fluid with a working depth of 14 cm and rotated until a nearly solid-body rotation was established. The flows in the tank were then generated by a bottomless cylinder placed vertically near the center of the tank and rotated in a clockwise direction. The frame supporting an electric motor with the cylinder on its axis was installed on the rotating table so that initially the cylinder was at rest with respect to the rotating tank. The cylinder was started from rest impulsively. This allowed us to reach the final rate of rotation of the cylinder $\Omega_1 = 0.4 - 0.9 \text{ s}^{-1}$ for a very short time (about 0.3 s) in the experiments with the Rossby numbers higher than critical. In some experiments, where the flow regime close to criticality was studied, the method of gradual increase of the rate of rotation with increments of 0.05 s^{-1} was employed. A sufficiently long time (about $5 - 10$ min) was allowed between the increments to be certain that almost steady flow was established. However, note that there were always some slow small-scale irregular motions, due to convection, for example, which were almost impossible to avoid in such a large tank. The space between the lower edge of the cylinder and the bottom of the tank was less than $0.3 - 0.4$ cm. The cylinder could be withdrawn vertically from the tank with the help of a sliding frame. Three cylinders of different radii ($R = 1.5$ cm, 3 cm, 5 cm) were employed in the sequence of experiments that we will report.

The working fluid consisted of a water solution of the pH indicator thymol-blue. This solution is of an orange-yellow color in its neutral state. For flow visualization a dc voltage was applied, so that the rotating cylinder constituted a negative electrode, whereas a copper plate at the side of the tank constituted a positive electrode. Due to the electrochemical reaction, the solution near the cylinder becomes basic and, as a result, changes the color to blue. Thus, a layer of dark blue fluid is formed around the cylinder, making the flow pattern visible and providing a good contrast for photography. A camera mounted above the tank or at the side of the tank in the rotating reference frame was employed to

record the patterns of dyed fluid that were formed by the flow. After each experiment it took only a few minutes for the diffusive chemical reaction with the acidic ambient fluid (an acid was added to the fluid in the tank) to restore the working fluid to its original yellow color.

III. BASIC FLOW AND STABILITY CONSIDERATIONS

Consider the evolution of the laminar flow that is induced by the cylinder of radius R rotating from time $t=0$ with angular velocity Ω_1 in a fluid initially at rest (in the rotating coordinate frame). Since the initial and boundary conditions do not depend on the polar angle θ , one can seek a solution with the same property. Note that the background rotation does not affect the velocity field in the case of purely two-dimensional flow. One can obtain the exact solution for this problem by solving the equations of motion, which in this case simply describe the viscous diffusion of vorticity. However, for the sake of simplicity, consider a self-similar flow induced by a point source of motion that illustrates the evolution of the actual flow induced by the cylinder of finite radius. We may imagine decreasing the radius R of the cylinder and simultaneously increasing Ω_1 such that the product $R^2\Omega_1$ remains constant. One then obtains (for details see, e.g., Voropayev and Afanasyev¹⁰) the respective distributions of the azimuthal velocity and vorticity for this flow:

$$v = \frac{\Gamma}{2\pi r} e^{-r^2/4\nu t}, \tag{1}$$

$$\omega = -\frac{\Gamma}{4\pi\nu t} e^{-r^2/4\nu t}, \tag{2}$$

where $\Gamma = 2\pi \lim_{R \rightarrow 0, \Omega_1 \rightarrow \infty} R^2\Omega_1$ is the intensity of the point source of motion. One may then note that a steady velocity distribution,

$$v = \frac{\Gamma}{2\pi r} = \frac{R^2\Omega_1}{r}, \tag{3}$$

will be established near the origin, while the velocity decays exponentially with distance for large r . The vorticity at a given r decays with time as $t^{-1}e^{-1/t}$.

Consider next the stability of a steady swirling flow in a rotating coordinate frame. The three components of the equation of motion written in the rotating frame of reference, together with the continuity equation, are, respectively,

$$\begin{aligned} \frac{\partial u}{\partial t} + (\mathbf{u} \cdot \nabla)u - \frac{v^2}{r} - 2\Omega_0 v \\ = -\frac{1}{\rho} \frac{\partial P}{\partial r} + \nu \left(\nabla^2 u - \frac{u}{r^2} - \frac{2}{r^2} \frac{\partial v}{\partial \theta} \right), \end{aligned} \tag{4}$$

$$\begin{aligned} \frac{\partial v}{\partial t} + (\mathbf{u} \cdot \nabla)v + \frac{uv}{r} + 2\Omega_0 v \\ = -\frac{1}{\rho} \frac{\partial P}{\partial \theta} + \nu \left(\nabla^2 v - \frac{v}{r^2} + \frac{2}{r^2} \frac{\partial v}{\partial \theta} \right), \end{aligned} \tag{5}$$

$$\frac{\partial w}{\partial t} + (\mathbf{u} \cdot \nabla)w = -\frac{1}{\rho} \frac{\partial P}{\partial z} + \nu \nabla^2 w, \tag{6}$$

$$\frac{\partial u}{\partial r} + \frac{u}{r} + \frac{1}{r} \frac{\partial v}{\partial \theta} + \frac{\partial w}{\partial z} = 0, \tag{7}$$

in which (u, v, w) are the components of the velocity vector \mathbf{u} in cylindrical coordinates (r, θ, z) and $P = p - \Omega_0^2 r^2 \rho / 2$ is a reduced pressure. Following the standard procedure (see, e.g., Chandrasekhar¹¹), we may consider the stability of a basic state flow that can be expressed in the following general form:

$$u = w = 0, \quad v = V(r) = r\Omega(r), \tag{8}$$

where $V(r)$ represents a solution of (4)–(7). One may then seek solutions for axisymmetric ($\partial/\partial\theta=0$) disturbances, periodic in the axial direction, of the form

$$(u', v', w', p') = (u, v, w, p)(r)e^{\gamma t} \cos kz, \tag{9}$$

where the perturbed state is described by $(u', V + v', w', p')$. Equations (4)–(7) then reduce to the following system of ordinary differential equations:

$$\nu(DD_* - k^2) - \gamma u + 2(\Omega + \Omega_0) = \frac{dp}{dr}, \tag{10}$$

$$\nu(DD_* - k^2) - \gamma v - 2(\Omega + \Omega_0) - r \frac{d}{dr} (\Omega + \Omega_0) = 0, \tag{11}$$

$$\nu(DD_* - k^2) - \gamma w = -kp, \tag{12}$$

$$D_* u = -kw, \tag{13}$$

in which

$$D = \frac{d}{dr}, \quad D_* = \frac{d}{dr} + \frac{1}{r}.$$

Note that for the inviscid problem, one may easily establish the stability criterion using the standard method of rewriting the equations in terms of Lagrangian variables. Rayleigh's stability criterion for the flow in nonrotating coordinates, determined in this way, then states that the flow is stable when the (Rayleigh) discriminant Φ is positive, a condition that has the explicit form

$$\Phi(r) = \frac{1}{r^3} \frac{d}{dr} (r^2 \Omega)^2 > 0.$$

In the case of interest herein, which concerns a flow in a rotating frame, the substitution $\Omega \rightarrow \Omega + \Omega_0$ leads directly to the more general stability criterion,

$$\Phi(r) = 2(\Omega + \Omega_0)(\omega + 2\Omega_0) > 0 \quad (\text{stability}). \tag{14}$$

Applying this criterion to the flow induced by the rotating cylinder, one immediately sees that when the cylinder rotates anticyclonically ($\Omega_0 > 0, \Omega_1 < 0$), then the flow is unstable when $|\Omega_1| > \Omega_0$ [the term in the first bracket in (14) becomes negative]. For a steady flow of the form (3), the width Δ of the annular region surrounding the cylinder in which the instability may develop is then given by

$$\Delta = R(\text{Ro}^{1/2} - 1), \tag{15}$$

where the Rossby number $\text{Ro} = |\Omega_1|/\Omega_0$ has been introduced. Note that when the cylinder rotates cyclonically

($\Omega_1 > 0$) the unsteady flow around the cylinder may still be unstable initially, since the vorticity is negative in this case and the term in the second bracket in (14) can be negative. However, since the absolute value of vorticity decreases with time, the flow restabilizes. As mentioned above, this is in accord with experimental observations.

Let us now return to the viscous problem. For consistency with the previous analyses for Couette flow, consider a flow between two coaxial cylinders of radii R (inner cylinder) and R_0 (outer cylinder). The general form of the stationary flow between the cylinders is

$$V = Ar + \frac{B}{r}. \tag{16}$$

Measuring r in units of the radius R_0 of the outer cylinder, writing $k^2 = a^2/R_0^2$, $\sigma^2 = \gamma R_0^2/\nu$, and making the transformation

$$\frac{2R_0^2}{\nu} (A + \Omega_0)u \rightarrow u,$$

and upon eliminating w and p , one obtains from (10)–(13) the system

$$(DD_* - a^2 - \sigma)(DD_* - a^2)u = -a^2 T' \left(\frac{1}{r^2} - \kappa' \right), \tag{17}$$

$$(DD_* - a^2 - \sigma)v = u, \tag{18}$$

in which

$$T' = -\frac{4B(A + \Omega_0)R_0^2}{\nu^2}, \quad \kappa' = -\frac{(A + \Omega_0)R_0^2}{B}.$$

In the case of interest to us here, $A = 0$ and $B = \Omega_1 R^2$, hence,

$$T' = -\frac{4\Omega_1 \Omega_0 R_0^2 R^2}{\nu^2}, \quad \kappa' = -\frac{R_0^2 \Omega_0}{R^2 \Omega_1}. \tag{19}$$

Equations (17) and (18) are formally the same as the equations for Couette flow in a nonrotating coordinate frame, except that the nondimensional governing parameters T' (Taylor number) and κ' are defined in a different manner. Introducing the radius ratio $\eta = R/R_0$, it is convenient to rewrite T' and κ' as $T' = T/\eta^2$, $\kappa' = \kappa/\eta^2$, where

$$T = -\frac{4\Omega_1 \Omega_0 R^4}{\nu^2}, \quad \kappa = -\frac{\Omega_0}{\Omega_1} = \text{Ro}^{-1}. \tag{20}$$

The appropriate boundary conditions for (17), (18) are that all components of the velocity vanish on the walls; thus,

$$u = v = 0, \quad Du = 0, \quad \text{for } r = 1 \quad \text{and } \eta, \tag{21}$$

where the last of the three boundary conditions is equivalent to $w = 0$.

If a basic state flow is unstable according to the criterion (14), one would expect viscous diffusion to have a stabilizing effect, in the sense that the flow would be stable for values of the Taylor number less than a certain critical value T_c . Thus, the problem is to determine T_c as a function of other governing parameters of the flow. There are a number of methods that have been developed for solving the system (17), (18) for the case of a narrow gap between cylinders.

However, in the case of interest here we are obliged to solve the system without making any assumptions about the width of the gap. The method based on the use of an expansion in terms of orthogonal cylindrical functions satisfying appropriate boundary conditions was developed (Chandrasekhar¹¹) for this problem for the case in which the marginal state is stationary ($\sigma = 0$). This method leads to a secular equation which allows one to determine numerically the minimal values of T' (as a function of a) for assigned values of κ' . We have performed the calculations in different approximations (from second to fourth order, the order of the approximation being the order of the determinant in the secular equation). The results are shown in the next section together with the experimental results.

Nonaxisymmetric disturbances can also be important in the dynamical evolution of the flow of interest to us here. Consider, for example, two-dimensional (barotropic) disturbances that depend upon the azimuthal angle θ , but not on the axial coordinate z . Since for purely two-dimensional flow (we assume that vertical motions are negligible) the background rotation does not play a role (the axis of rotation being perpendicular to the plane of motion), the well-known inflexion-point theorem of Rayleigh can be applied. An analog of this theorem for circular flows (e.g., Drazin and Reid¹²) states that a necessary condition for instability with respect to two-dimensional disturbances is that the gradient of the basic vorticity,

$$D\omega = D \frac{1}{r} D(rV), \tag{22}$$

must change sign. Obviously $D\omega \equiv 0$ when V is of the form (16), and it has been shown for Couette flow that there are no unstable modes in the spectrum for this flow. However, two-dimensional barotropic disturbances can develop if the basic flow is altered by the primary axisymmetric disturbances. Consider the azimuthal velocity profile in the flow around the rotating cylinder where axisymmetric disturbances due to the centrifugal instability evolve in an annulus of width Δ (15). An inviscid form of Eq. (5) written for axisymmetric motions implies the following conservation law:

$$\frac{D}{Dt} (rV + r^2 \Omega_0) = 0, \tag{23}$$

where D/Dt is the material derivative. According to this relation a fluid particle moving radially from the wall of the rotating cylinder to some radius r , acquires the azimuthal velocity

$$v' = \frac{1}{r} [\Omega_1 R^2 - \Omega_0 (r^2 - R^2)]. \tag{24}$$

Suppose that in the annular region within which axisymmetric centrifugal disturbances amplify, the distribution of velocity is given by (24). Since outside the annulus the velocity is of the form (3), there should be some transition region at the periphery of the annulus. The distribution of velocity in the transition region is shown schematically in Fig. 2. One may then obtain a vorticity distribution such that the gradient of the vorticity changes sign somewhere at the periphery of

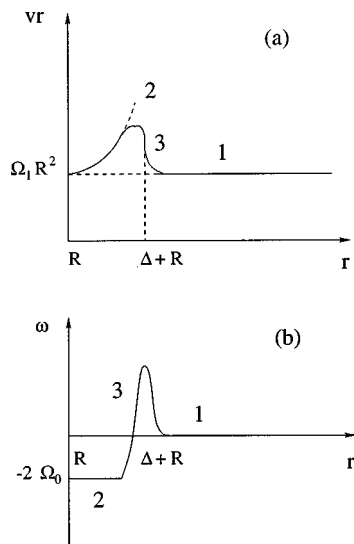


FIG. 2. Radial distribution of the circulation vr (a) and vorticity ω (b) for the flow altered by radial motions due to the centrifugal instability. The curves labeled 1,2 represent distributions (3) and (24), respectively, while 3 is intended to represent a transitional distribution.

the annulus. Thus, two-dimensional barotropic Kelvin–Helmholtz-type instability may develop as a consequence of the primary centrifugal instability of the basic flow. In the next section we will, in fact, demonstrate that both types of instability are realized experimentally.

IV. EXPERIMENTAL RESULTS AND INTERPRETATION

A typical evolution of the unstable flow induced by the rotating cylinder is illustrated by the photographs shown in Figs. 3, 4, and 5. After the cylinder is set in motion, the circular bands of dyed fluid appear around the cylinder with a well-defined vertical wave number. Toroidal vortices of mushroom-like shape in the cross section then grow from these bands. They form in the annular region surrounding the cylinder in which the instability is initiated. Since the radial motions due to the centrifugal instability change the radial distribution of the azimuthal velocity of the basic flow, a secondary Kelvin–Helmholtz-type instability develops at the periphery of the unstable annulus, thus creating a complex three-dimensional flow [Figs. 4(a), 5(b)]. In an oblique view of the flow (Fig. 6), typical Kelvin–Helmholtz-like vortices are clearly visible in the horizontal plane. Flows with azi-

muthal wave numbers in the range from two to six were observed for different values of Rossby and Reynolds numbers. If the rotating cylinder is carefully withdrawn vertically from the fluid, one gets a vortex with an initially stable core rotating like a solid body and a boundary layer outside. The perturbations introduced by the withdrawal of the cylinder together with centrifugal instability give rise to the Kelvin–Helmholtz-type instability. It is this instability initiated at the periphery of the vortex that rapidly erodes the vortex core (Fig. 7) in a way that is consistent with the behavior of unstable vortices produced by stirring the fluid inside a cylinder in the previous laboratory experiments by Kloosterziel and van Heijst.⁸

The vertical wavelength of the primary instability was measured in our experiments as a function of the Rossby number Ro . The results for three cylinders of different radii are presented in Fig. 8. The fact that the experimental data for different cylinders do not collapse onto a single curve indicates that the nondimensional wavelength λ/R obviously depends not only on Ro but also on the Reynolds number Re , which can be defined as

$$Re = \frac{R^2 \Omega_1}{\nu},$$

since the values of Re in the experiments differ for different cylinders ($Re=110$ – 220 for the cylinder of radius $R=1.5$ cm, $Re=450$ – 900 for $R=3$ cm, $Re=1250$ – 2500 for $R=5$ cm). The behavior of λ/R for large Ro suggests a power law relation of the form

$$\lambda/R = Re^{-1/2} f(Ro). \quad (25)$$

Normalized values of λ were therefore plotted (Fig. 9) as a function of Ro in order to illustrate the validity of the relation (25).

The width of the unstable annulus was also estimated as the maximum radial dimension of the mushroom-like vortices. The results presented in Fig. 10 again reveal the dependence on the Reynolds number. The measured width of the annulus for the small cylinder ($R=1.5$ cm) is in good agreement with the values predicted by (15) for the entire range of Ro . Since the Reynolds number is smallest in this case the role of viscosity in the flow is relatively important and the basic velocity profile (3), which is established only in consequence of the viscous diffusion of momentum, has a chance to form prior to the onset of the instability that sig-

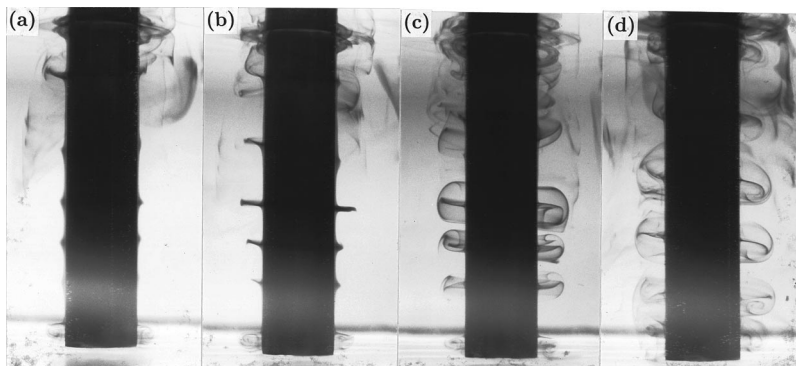


FIG. 3. A sequence of photographs showing the evolution of the centrifugal instability. Side view. Experimental parameters: $R=1.5$ cm, $Ro=3.4$, $Re=150$; $t=10$ s (a), $t=12$ s (b), $t=15$ s (c), $t=18$ s (d).

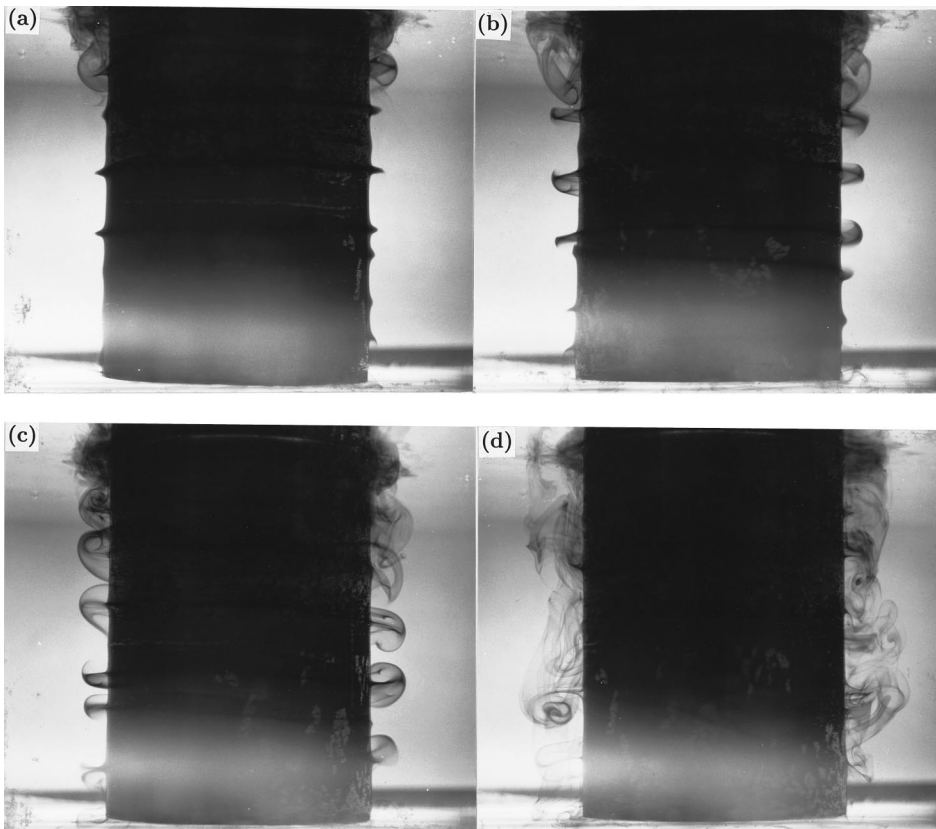


FIG. 4. A sequence of photographs showing the evolution of the centrifugal instability. Side view. Experimental parameters: $R=5$ cm, $Ro=2.5$, $Re=2000$; $t=5$ s (a), $t=7$ s (b), $t=9$ s (c), $t=11$ s (d).

nificantly alters the basic state flow. Although vortices may, in general, extend outside the boundary layer (as, e.g., in the case of Görtler vortices), this is not the case in our experiment, since the radial dimension of the vortices is smaller than the theoretical estimate. This provides assurance that the dimension of the vortices may provide a reasonable estimate of the width of the boundary layer.

The second series of experiments that we performed were specifically designed to enable us to measure the critical Taylor number T_c as a function of the other governing parameter, the Rossby number Ro . These experiments were initiated with the absolute value of the rotation rate of the cylinder set to a value just slightly greater than the background rotation rate, i.e., $|\Omega_1| > \Omega_0$. Then $|\Omega_1|$ was incremented until the flow became centrifugally unstable. On this basis, the critical values of Ω_1 were determined and the values of T_c given by (20) thereafter calculated. These results

are shown as a function of $\kappa = Ro^{-1}$ in Fig. 11, together with the theoretical curves obtained by solving (17) and (18) for a stationary marginal state using Chandrasekhar's method. The values of η that represent the boundary conditions (21) for the problem, were chosen to fit with the experimental data for each cylinder. For this purpose, the dependence of $T_c(\kappa=0)$ upon η was calculated (Fig. 12). The approximate values of $T_c(\kappa=0)$ suggested by the extrapolation of experimental data were then used to obtain the values of η from the relationship of Fig. 12. These values of η were in turn employed to calculate the curves presented in Fig. 11. The values of η thereby obtained give the effective width of the annulus in which the perturbations appear initially as

$$\Delta' = R(\eta^{-1} - 1),$$

which is about 1 cm for all cylinders. Since the entire pro-

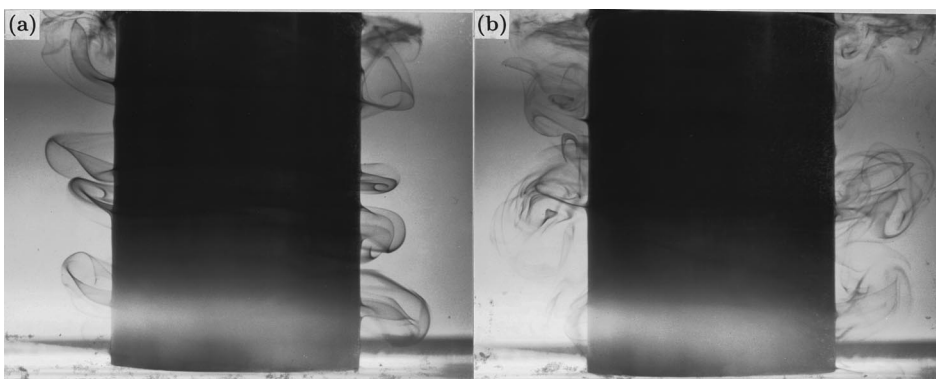


FIG. 5. The same as in Fig. 4 but for an increased value of the Rossby number $Ro=5.9$; $t=5$ s (a); $t=7$ s (b).

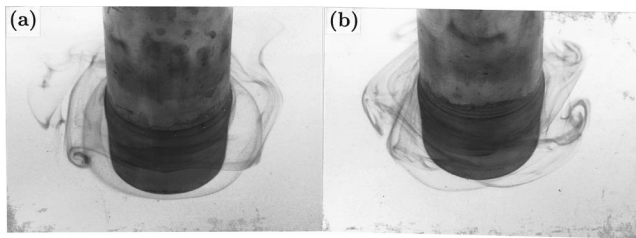


FIG. 6. Kelvin-Helmholtz-type vortices at the periphery of the unstable annulus.

cess is transient in the sense that the onset of instability takes place simultaneously with basic state flow development, one might reasonably expect that the instability could develop for smaller values of T_c if one were to wait for a sufficiently long time that the annular region in which the velocity profile (3) is established, becomes wider (η becomes smaller). However, this scenario is not realizable. Since $T_c \propto \Omega_0 \Omega_1$ and $|\Omega_1|$ is always greater than Ω_0 , one can make T_c smaller by decreasing the rotation rate Ω_0 of the experimental tank. However, when the tank rotates very slowly, the three-dimensional background irregular motions (which always exist in the tank) do not decay since they are not suppressed by the background rotation (i.e., the Rossby number for these motions is not sufficiently small). This background turbulence then creates the effective initial conditions for the perturbations by not allowing the annulus to become sufficiently wide prior to the onset of the instability. The vertical wavelength λ_c of the perturbations at the onset of instability (when $T \approx T_c$) was also measured in the experiments. The values of λ_c/R as a function of η are shown in Fig. 13 together with the theoretical curve, which represents the calculated values of the wavelength for $T = T_c$ at $\kappa = 0$.

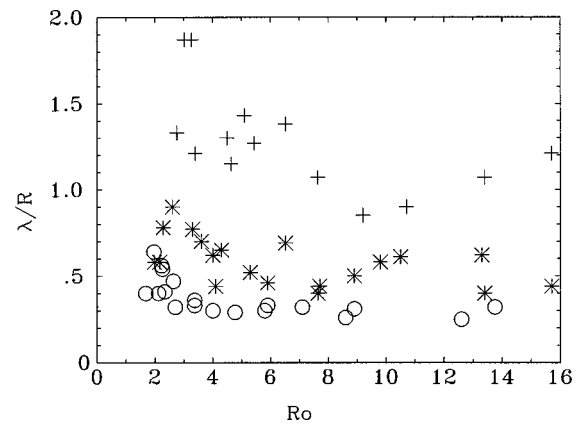


FIG. 8. Nondimensional vertical wavelength of the perturbations for different values of the Rossby number. Different symbols indicate the experimental data for different cylinders: (+) $R = 1.5$ cm; (*) 3 cm; (O) 5 cm.

V. DISCUSSION AND CONCLUSIONS

It is interesting to compare, at least qualitatively, our experimental results with those for Couette flow as well as with numerical results for the centrifugal destabilization of anticyclonic barotropic columnar vortices. Note that not only toroidal but also spiral vortices (Fig. 14) were observed in our experiments when the large cylinder ($R = 5$ cm) was employed, and hence the Reynolds number was largest. This is consistent with a well-known flow regime diagram (see Fig. 2 in Andereck *et al.*¹³) for counter-rotating cylinders, where observations of Taylor (toroidal) vortices have been documented for smaller values of the Reynolds number while spiral vortices are observed for larger values of the Reynolds number. Since the primary aim of our experiments was to demonstrate the appearance of centrifugal instability of a vortex in a rotating fluid with a possible application to atmospheric vortices rather than to present another example of

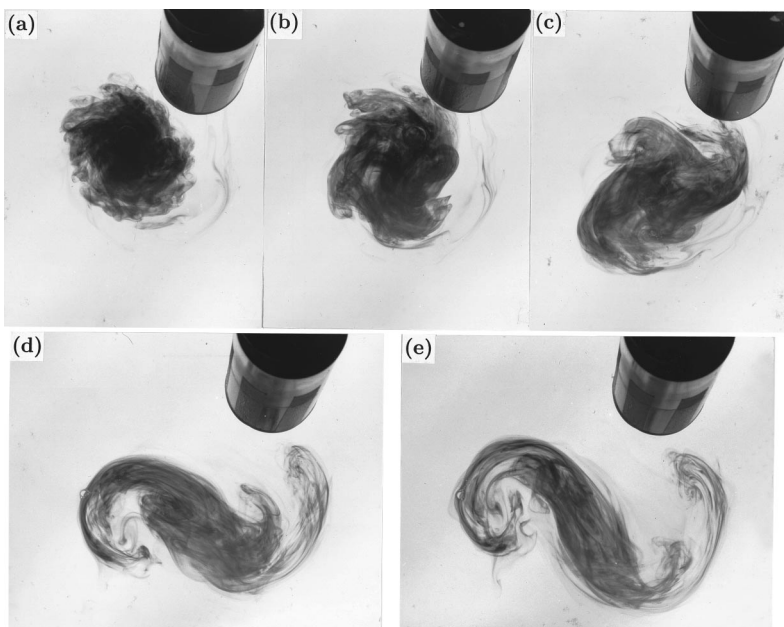


FIG. 7. A sequence of photographs showing the evolution of the vortex after the cylinder was withdrawn from the water. Top view. Experimental parameters: $R = 3$ cm, $Ro = 3.8$, $Re = 700$.

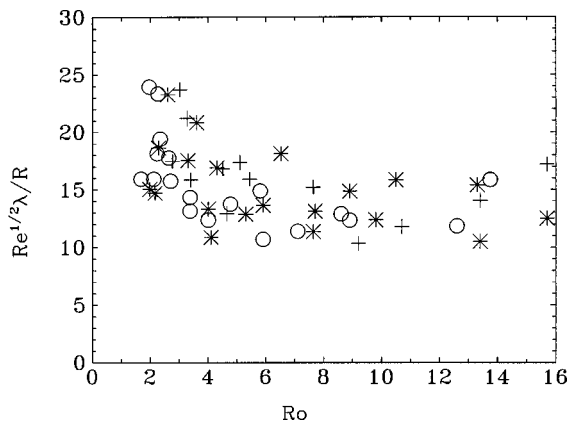


FIG. 9. Normalized values of the vertical wavelength versus the Rossby number. The symbols are the same as in Fig. 8.

Taylor-vortex flow, we did not follow the routine that has become standard for Couette flow experiments. Since the typical aspect ratio of the atmospheric vortices of interest is not large, we did not try to model a vortex of infinite height in our experiments. However, the typical ratio of wavelength of primary instability to the depth of the fluid is not particularly small in our experiments, $\lambda/H=5-8$ for the small cylinder ($R=1.5$ cm) and 7–11 for the large cylinder ($R=5$ cm). Note that in the experiments on flow regimes in the Couette system by Andereck *et al.*,¹³ the typical value of $\lambda/H=15$. Obviously finite-length effects will play some role in our experiments, although their influence cannot be determinant. For example, due to the vortex-number quantization condition (Park and Donnelly¹⁴) the number of vortices may vary in such a way as to contribute to the scatter of experimental data. The Ekman cells of height 0.5–1 cm adjacent to the top and bottom boundaries can also be detected in our system. Regarding the critical Taylor number, we may refer to the experiments of Cole¹⁵ who has shown that the value of T_c at which axisymmetric Taylor vortex flow occurs is rather insensitive to annulus length. Having in mind the nonuniqueness of the stable flow states in the Couette system demonstrated by Coles,¹⁶ we have followed a certain path (though not a so-called thermodynamic path) in parameter space, the

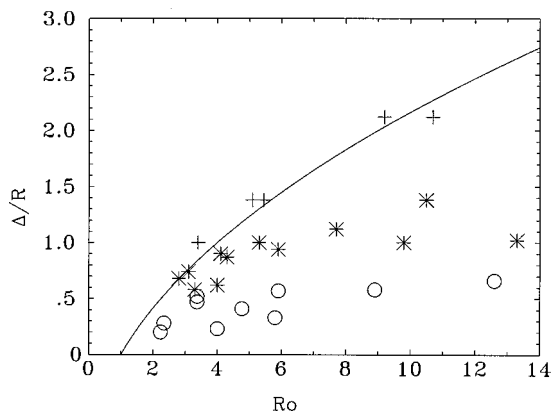


FIG. 10. The nondimensional width of the unstable annulus for different values of the Rossby number. The symbols are the same as in Fig. 8. The solid line represents the relationship (5).

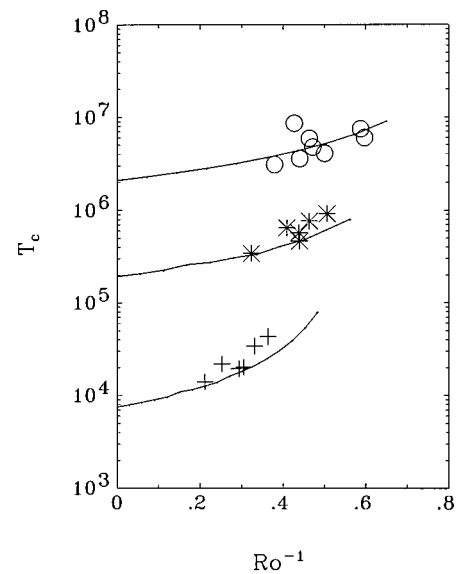


FIG. 11. Critical values of the Taylor number as a function of the inverse Rossby number. Solid lines represent the solutions of (17), (18) for a stationary marginal state with different boundary conditions ($\eta=0.85, 0.75, 0.55$). The symbols are the same as in Fig. 8.

same path in all experiments: first the state of solid-body rotation was established and then the cylinder was started from rest impulsively. An important feature of the flows in our experiments is that they are, in fact, strongly unsteady due to the continuous viscous diffusion of momentum from the cylinder (the process that establishes the basic flow) and also due to the simultaneous development of toroidal vortices (primary instability) together with the barotropic Kelvin–Helmholtz-like vortices (secondary instability). The development of these instabilities leads finally to a fully turbulent flow. Thus, a steady state with embedded toroidal vortices is never achieved in this case as it would be in conventional Couette flow. This explains the pronounced complexity of

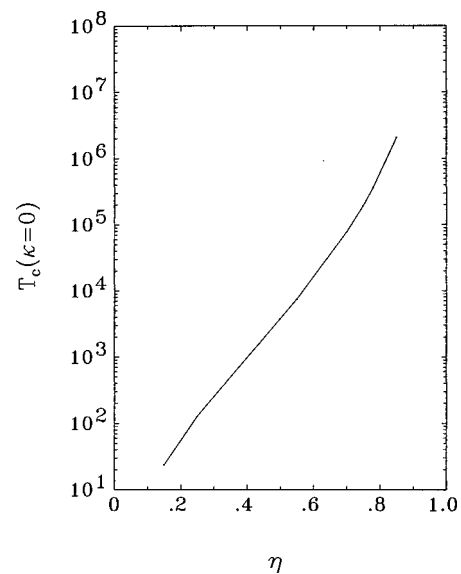


FIG. 12. Calculated values of the critical Taylor number at $\kappa=0$ for different values of the boundary parameter η .

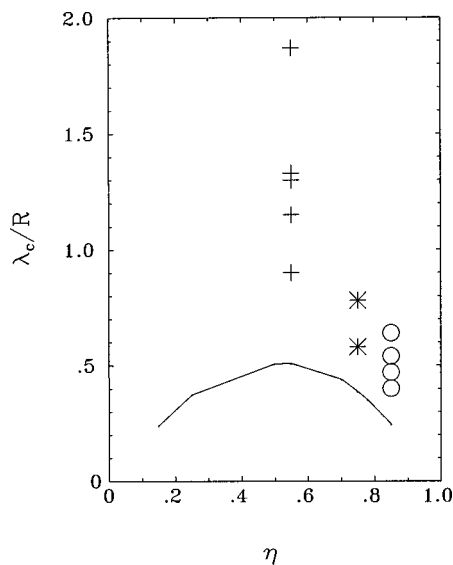


FIG. 13. The nondimensional wavelength of perturbations measured in the experiments where the Taylor numbers were near their critical values. The values of η are the same as in Fig. 11. The solid curve represents the calculated values of λ_c for $T=T_c$ and $\kappa=0$.

the flow of interest for us (e.g., Figs. 3–5) as well as the rather significant deviation of the experimental points from the theoretical curve in Fig. 13. Note that it is the impulsive start that allows us to reach the final, though unsteady, state with highly supercritical values of the Rossby number. Otherwise, if gradual increments of rotation rate were employed, one would necessarily pass through a succession of intermediate unstable states and the final result would be uninteresting, since the flow would become turbulent (due to the secondary Kelvin–Helmholtz-like instability) well before the final value of the Rossby number could be reached.

The Smyth and Peltier¹ numerical results on the growth rate of three-dimensional perturbations in the case of centrifugal instability (their so-called edge mode) of anticyclonic vortices on the f -plane show [see Fig. 13(b) in their paper], demonstrate that the instability is not especially selective in terms of the vertical wavelength of the amplified perturbations so that a wide spectrum of motions can be realized. This explains the large scatter of the data shown in Fig. 8. Note that in spite of the fact that the basic flows are different, our results can be related to those of Smyth and Peltier if one takes the width of the annulus, wherein instability occurs, as a natural characteristic length scale for both cases. The maximum growth of perturbations was found for the value of nondimensional vertical wave number $d=2$ and Rossby number $Ro=3.3$. The distribution of the kinetic energy of the perturbation (Fig. 16 in Smyth and Peltier¹) locates the annular region in which the perturbation is local-

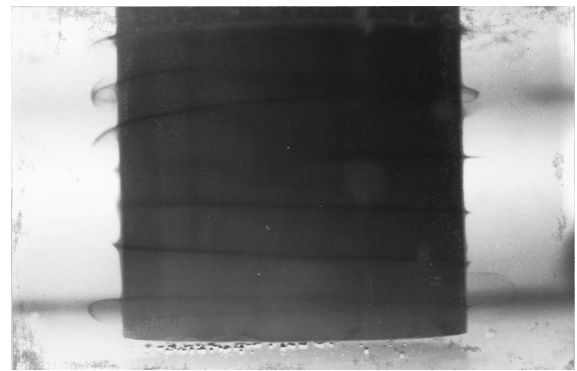


FIG. 14. Typical spiral vortices observed in the experiment with a large Reynolds number ($Re=2500$).

ized. On this basis one may estimate the ratio of the horizontal scale of the perturbation to the vertical scale. For $d=2$, this ratio is near 0.7 while in our experiments the ratio Δ/λ varies between 1 and 2 for different values of Ro . We are therefore justified in concluding that our experiments have successfully captured the essence of the “edge-mode” of centrifugal instability to which anticyclonic columnar vortices are susceptible for Rossby numbers of $O(1)$.

- ¹W. D. Smyth and W. R. Peltier, “Three-dimensionalization of barotropic vortices on the f -plane,” *J. Fluid Mech.* **265**, 25 (1994).
- ²G. F. Carnevale, M. Briscolini, R. C. Kloosterziel, and G. K. Vallis, “Three-dimensionally perturbed vortex tubes in a rotating flow,” *J. Fluid Mech.* **341**, 127 (1997).
- ³P. G. Potylitsin and W. R. Peltier, “Stratification effects on the stability of barotropic vortices on the f -plane,” *J. Fluid Mech.* **355**, 45 (1998).
- ⁴M. Lesieur, S. Yanase, and O. Metais, “Stabilizing and destabilizing effects of a solid-body rotation on quasi-two-dimensional shear layers,” *Phys. Fluids A* **3**, 403 (1991).
- ⁵P. Bartello, O. Metais, and M. Lesieur, “Coherent structures in rotating three-dimensional turbulence,” *J. Fluid Mech.* **273**, 1 (1994).
- ⁶P. H. Alfredsson and H. Persson, “Instabilities in channel flow with system rotation” *J. Fluid Mech.* **202**, 543 (1989).
- ⁷A. A. Bidokhti and D. J. Tritton, “The structure of a turbulent free shear layer in a rotating fluid,” *J. Fluid Mech.* **241**, 469 (1992).
- ⁸R. C. Kloosterziel and G. J. F. van Heijst, “An experimental study of unstable barotropic vortices in a rotating fluid,” *J. Fluid Mech.* **223**, 1 (1991).
- ⁹S. Leblanc and C. Cambon, “On the three-dimensional instabilities of plane flows subjected to Coriolis force,” *Phys. Fluids* **9**, 1307 (1997).
- ¹⁰S. I. Voropayev and Y. D. Afanasyev, *Vortex Structures in a Stratified Fluid* (Chapman and Hall, London, 1994).
- ¹¹S. Chandrasekhar, *Hydrodynamic and Hydromagnetic Stability* (Dover, New York, 1981).
- ¹²P. G. Drazin and W. H. Reid, *Hydrodynamic Stability* (Cambridge University Press, Cambridge, 1991).
- ¹³C. D. Andereck, S. S. Liu, and H. L. Swinney, “Flow regimes in a circular Couette system with independently rotating cylinders,” *J. Fluid Mech.* **164**, 155 (1986).
- ¹⁴K. Park and R. J. Donnelly, “Study of the transition to Taylor vortex flow,” *Phys. Rev. A* **24**, 2277 (1981).
- ¹⁵J. A. Cole, “Taylor-vortex instability and annulus-length effects,” *J. Fluid Mech.* **75**, 1 (1976).
- ¹⁶D. Coles, “Transition in circular Couette flow,” *J. Fluid Mech.* **21**, 385 (1965).